Chaos, Solitons and Fractals 106 (2018) 310–316

Contents lists available at ScienceDirect

Chaos, Solitons and Fractals

Nonlinear Science, and Nonequilibrium and Complex Phenomena

journal homepage: www.elsevier.com/locate/chaos

Nonlinear dynamics behind the seismic cycle: One-dimensional phenomenological modeling

Srđan Kostić[a,*], Nebojša Vasović[b], Kristina Todorović[c], Igor Franović[d]

[a] Department for Scientific Research and Informatics, Institute for Development of Water Resources "Jaroslav Černi", Jaroslava Černog 80, Belgrade 11226, Serbia
[b] Department of Applied Mathematics, University of Belgrade Faculty of Mining and Geology, Serbia
[c] Department of Physics and Mathematics, University of Belgrade Faculty of Pharmacy, Serbia
[d] Scientific Computing Lab, University of Belgrade, Institute of Physics, Serbia

ARTICLE INFO

Article history:
Received 12 July 2017
Revised 27 November 2017
Accepted 30 November 2017

Keywords:
Spring-block model
Time delay
Rate-and-state dependent friction law
Seismic cycle

ABSTRACT

In present paper, authors examine the dynamics of a spring-slider model, considered as a phenomenological setup of a geological fault motion. Research is based on an assumption of delayed interaction between the two blocks, which is an idea that dates back to original Burridge–Knopoff model. In contrast to this first model, group of blocks on each side of transmission zone (with delayed interaction) is replaced by a single block. Results obtained indicate predominant impact of the introduced time delay, whose decrease leads to transition from steady state or aseismic creep to seismic regime, where each part of the seismic cycle (co-seismic, post-seismic and inter-seismic) could be recognized. In particular, for coupling strength of order 10^2 observed system exhibit inverse Andronov–Hopf bifurcation for very small value of time delay, $\tau \approx 0.01$, when long-period ($T = 12$) and high-amplitude oscillations occur. Further increase of time delay, of order 10^{-1}, induces an occurrence of a direct Andronov–Hopf bifurcation, with short-period ($T = 0.5$) oscillations of approximately ten times smaller amplitude. This reduction in time delay could be the consequence of the increase of temperature due to frictional heating, or due to decrease of pressure which follows the sudden movement along the fault. Analysis is conducted for the parameter values consistent with previous laboratory findings and geological observations relevant from the seismological viewpoint.

1. Introduction

It is generally considered that process of accumulation and release of stress along the seismogenic faults always obeys the same rule: period with no movement along the fault (or with aseismic creep), when the stress is being accumulated, is followed by its sudden release, which could be further succeeded by the partial emission of the remained stored energy. These three periods, formally known as inter-seismic, co-seismic and post-seismic, respectively, constitute a single seismic cycle, which could be manifested at regular time intervals (for the strongest seismic events), or, more likely, occurrence of seismic events appears as a random process following Poisson distribution [1]. From the seismological viewpoint previous studies on properties of a seismic cycle resulted in sufficiently accurate characterization of each of the aforementioned periods. It is well known that inter-seismic deformation indicates depth of the zone that will eventually rupture seismically [2] and the rate at which stress is accumulating along the fault zone [3]. The very end of this inter-seismic period could be marked by the occurrence of foreshocks as small partial releases of the stored potential energy before the main event. On the other hand, post-seismic deformation is usually driven by the preceding co-seismic stress change [3] and it could be as large as the fault slip during the main seismic event. Observed post-seismic behavior includes poroelastic deformation [4], frictional afterslip [5] and viscoelastic relaxation [6]. Similarly to the inter-seismicposteriod, post-seismic part of the seismic cycle could be marked by the occurrence of aftershocks, as sudden releases of the remaining stored energy with significantly smaller magnitude in comparison to the main seismic event.

From the purely mechanical viewpoint, it is commonly considered that alternation of seismic cycles could be described by irregular stick-slip behavior [7]. For a simple frictional system, like commonly used spring-block model, the occurrence of stick-slip is due to a difference in static and kinetic friction, i.e. once the block starts to slide the friction drops suddenly to a lower level [8]. It is generally considered that surface roughness and normal

* Corresponding author.
E-mail address: srdjan.kostic@jcerni.co.rs (S. Kostić).

https://doi.org/10.1016/j.chaos.2017.11.037

stress level play main role in "pushing" the spring-block model into stick-slip regime [9]. In present analysis, we analyze only the effect of friction on dynamics of spring-block model, by assuming some small constant value of normal stress which does not significantly affect the dynamics of the model. This could correspond to shallow parts of the Earth's crust, or parts where horizontal stresses are much higher that vertical ones, due to significant effect of tectonics and surface erosion which reduced the thickness of the overlying layers.

Results of the pioneer work of Burridge and Knopoff [10] on dynamics of a simple spring-block model set a solid base for succeeding laboratory and theoretical research of seismogenic fault motion. The main outcome of their work is that distribution of displacement sums (i.e. earthquake magnitudes) follows two key macrosesimologic laws: Gutenberg–Richter and Omori–Utsu power law distribution. This finding enabled succeeding researchers a wide specter of additional analyzes, from the purely seismological [11,12], across the tribological [13,14] to purely dynamical [15]. These "dynamical" research are primarily in our focus, since they showed that for a certain parameter range, dynamics of spring-block models exhibit a regular transition between different dynamical regimes, with the eventual occurrence of chaotic dynamics [16,17]. Nevertheless, former studies did not treat the problem of seismic cycle *per se*, except from our previous paper, where we analyzed the impact of transient seismic wave on the dynamics of spring-block model, which resulted in transition between different seismic cycles [18]. One of the goals of the present analysis is to match different dynamical regimes of a spring-block model to appropriate phases of seismic cycles. In particular, the performed analysis should provide answers to the following questions: (1) what are the relevant parameter ranges for which the dynamic of the spring-block model enters the stick-slip regime, (2) what are the main dynamical features of that regime and (3) what does it mean for the real conditions in Earth's crust. In that way, we will be able to reveal the main controlling mechanism behind the regularity of seismic cycle. One should note that, besides seismology, nonlinear models in general have been successively applied in other areas of natural sciences, as well [19–24].

Besides the analogy with the macroseismological laws, another important outcome of the original work of Burridge and Knopoff concerns a delayed transition of motion among two sets of blocks, indicating possible highly complex dynamical behavior. In particular, they showed that displacement among two boundary group of blocks in an one-dimensional chain is being transmitted with a certain time delay, whose order of unit corresponds to the viscosity of the middle set of blocks. Although this finding opened a lot of possibilities for investigating the cause and consequences of such a feature, it was not taken into consideration in succeeding studies. Effect of time delay was previously only implicitly introduced in friction term [25,26], and between the neighboring blocks in an one-dimensional chain of blocks with rate-dependent friction law [27]. In present paper, we analyze the transition between different seismic cycles considering the delayed interaction among the blocks with a rate-and state-dependent friction law. In contrast to our previous work, delayed interaction is assumed between the blocks exhibiting rate-and state-dependent friction law, which corresponds well to the laboratory observations of rock friction. Also, present analysis is conducted for the values of parameters which are either observed in reality or in laboratory conditions. We consider that this behavior is also relevant from the viewpoint of seismology, since different friction conditions along the fault (e.g. different thickness and physico-mechanical properties of fault gouge, impact of pore fluid, etc.) could cause a delayed transition of motion among different parts of the active seismogenic fault.

To sum up, the main idea of the present study is to determine the main dynamical mechanism by which the fault motion model reaches stick-slip like oscillations, as an appropriate dynamical state of a seismic fault motion which includes the interseismic, co-seismic and post-seismic regime. Thereby, dynamics of the relevant model is examined for the parameter values meaningful from the viewpoint of seismology, under the influence of the assumed delayed interaction of variable strength. Introduction of new influential parameters is motivated by the previous laboratory findings, with the aim of modeling the effect of changeable friction properties along the fault. The analysis is conducted using both analytical and numerical methods, former of which involved the application of local bifurcation analysis for the model with constant time delay whose results are corroborated numerically.

2. Model development

2.1. Original model of fault motion

Our numerical simulations of a spring-block model are based on the system of equations coupled with Dieterich–Ruina rate-and state-dependent friction law [16]:

$$
\begin{aligned}
\dot{\theta} &= -\left(\frac{\nu}{L}\right)\left(\theta + B\log\left(\frac{\nu}{\nu_0}\right)\right) \\
\dot{u} &= \nu - \nu_0 \\
\dot{\nu} &= \left(-\frac{1}{M}\right)\left(ku + \theta + A\log\left(\frac{\nu}{\nu_0}\right)\right)
\end{aligned}
\tag{1}
$$

where parameter M is the mass of the block and the spring stiffness k corresponds to the linear elastic properties of the rock mass surrounding the fault [28]. According to Dieterich and Kilgore [29] the parameter L corresponds to the critical sliding distance necessary to replace the population of asperity contacts. The parameters A and B are empirical constants, which depend on material properties. Variables u and ν represent displacement and velocity, while θ denotes the state variable describing the state of the rough surface along which blocks are moving [30]. Parameter V_0 represents the constant background velocity of the upper plate Fig. 1). For convenience, system ((2) is non-dimensionalized by defining the new variables θ', v', u' and t' in the following way: $\theta = A\theta'$, $v = v_0 v'$, $u = Lu'$, $t = (L/v_0)t'$, after which we return to the use of θ, v, u and t. This non-dimensionalization puts the system into the following form:

$$
\begin{aligned}
\dot{\theta} &= -\nu(\theta + (1+\varepsilon)\log(\nu)) \\
\dot{u} &= \nu - 1 \\
\dot{\nu} &= -\gamma^2[u + (1/\xi)(\theta + \log(\nu))]
\end{aligned}
\tag{2}
$$

where $\varepsilon = (B-A)/A$ measures the sensitivity of the velocity relaxation, $\xi = (kL)/A$ is the nondimensional spring constant, and $\gamma = (k/M)^{1/2}(L/v_0)$ is the nondimensional frequency [16]. As it was previously shown [18], a supercritical direct Andronov–Hopf bifurcation curve occurs for the following parameter values $\varepsilon = 0.27$, $\xi = 0.5$ and $\gamma = 0.8$, leading from equilibrium state to regular periodic oscillations.

2.2. Fault motion model under study

We analyze the dynamics of two coupled blocks Fig. 1), whose motion is governed by the following system of first-order ordinary

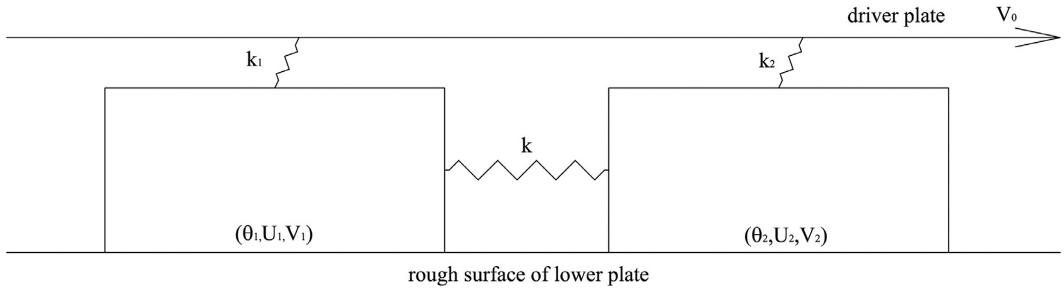

Fig. 1. Setup of the analyzed model.

differential equations, starting from the original system (1):

$$\begin{aligned}
\dot{\theta}_1 &= -\left(\frac{V_1}{L_1}\right)\cdot\left(\theta_1 + B_1 \ln\left(\frac{V_1}{V_0}\right)\right)\\
\dot{U}_1 &= V_1 - V_0\\
\dot{V}_1 &= (-1/M_1)[k_1U_1 - k(U_2(t-\tau) - U_1(t)) + \theta_1 + A_1 \ln(V_1/V_0)]\\
\dot{\theta}_2 &= -\left(\frac{V_2}{L_2}\right)\cdot\left(\theta_2 + B_2 \ln\left(\frac{V_2}{V_0}\right)\right)\\
\dot{U}_2 &= V_2 - V_0\\
\dot{V}_2 &= (-1/M_2)[k_2U_2 - k(U_1(t-\tau) - U_2(t)) + \theta_2 + A_2 \ln(V_2/V_0)]
\end{aligned} \tag{3}$$

Here we introduced time delay between the two coupled blocks. In this way, we simulate the original model of Burridge and Knopoff [10], where two blocks actually represent two boundary sets of blocks, and the effect of the middle set of blocks (with different viscosity properties in comparison to other two sets) is replicated by the delayed interaction between the two blocks.

Appropriate non-dimensionalization puts the system (3) into the following form:

$$\begin{aligned}
\dot{\theta}_1 &= -V_1\cdot(\theta_1 + (1+\varepsilon_1)\ln V_1)\\
\dot{U}_1 &= V_1 - 1\\
\dot{V}_1 &= \gamma_1^2\left(-U_1 + c_1(U_2(t-\tau) - U_1(t)) - \left(\frac{1}{\xi_1}\right)(\theta_1 + \ln(V_1))\right)\\
\dot{\theta}_2 &= -V_2\cdot(\theta_2 + (1+\varepsilon_2)\ln V_2)\\
\dot{U}_2 &= V_2 - 1\\
\dot{V}_2 &= \gamma_2^2\left(-U_2 + c_2(U_1(t-\tau) - U_2(t)) - \left(\frac{1}{\xi_2}\right)(\theta_2 + \ln(V_2))\right)
\end{aligned} \tag{4}$$

where $c_i = k/k_i$, $i = 1,2$; $\theta_{1new} = \theta_{1old}/A$, $V_{new} = V_{old}/V_0$, $U_{new} = U_{old}/L$, $t_{new} = (L/V_0)t_{old}$, $\varepsilon = (B-A)/A$, $\xi = (kL)/A$, $\gamma = (k/M)^{1/2}(L/V_0)$. In present paper, we consider that $\varepsilon_1 = \varepsilon_2 = \varepsilon$, $\gamma_1 = \gamma_2 = \gamma$, $\xi_1 = \xi_2 = \xi$ and $c_1 = c_2 = c$.

3. Choice of the relevant parameter values

As it is commonly known, dynamics of any system is predominantly controlled by an action of a few control parameters, whose tuning induce corresponding transitions between different dynamical regimes. Thereby, variations of control parameters should be performed within the relevant intervals, i.e. by taking the parameter values which are of interest either from theoretical viewpoint, or which are observed in laboratory conditions or *in situ*.

Original model (2) has three main control parameters that predetermine its dynamics. As it was previously indicated, parameter ε denotes the ratio of stress drop and stress increase during the fault motion (Fig. 2). According to the results of previous studies [5], this ratio needs to be positive in order to capture the velocity-weakening behavior, i.e. for (B–A) > 0 one could observe the unstable dynamics relevant from the viewpoint of seismology. Previous research showed that this condition is fulfilled at depths in Earth's crust where the most crustal earthquake foci are located, approximately between 5 and 15 km [5]. Below and above this zone, parameter ε has negative values, indicating velocity-strengthening behavior, which secures the stable dynamics of fault motion. Regarding the relevant values of parameter ε, preceding laboratory findings on friction properties of granite samples (since continental crust is mostly composed of granite) indicated that parameters A and B are of the order of magnitude 10^{-3} [31], with ratio (B–A)/A in the interval [−0.17,0.36], which indicates that meaningful values of ε could be taken from the interval [−1,1] (Table 1). One should note that present analysis is constrained only to the dynamics of crustal faults, since fault motion in the subduction zones is under prevailing gravitational influence, which is not examined in this study. It should also be emphasized that in present analysis we observe only the velocity weakening behavior, so negative values of dimensionless stress ratio are not examined.

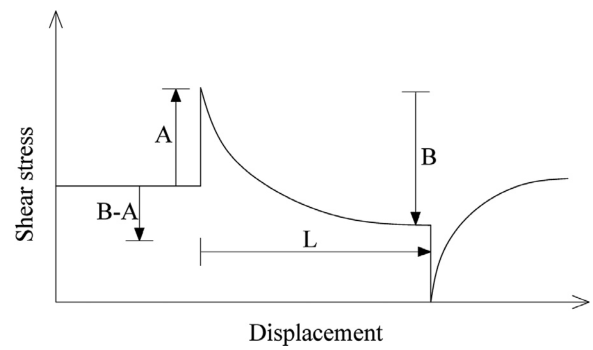

Fig. 2. General scheme of a shear stress variation during the motion of analyzed model shown in Fig. 1.

Parameter ξ is defined as a function of spring stiffness k_L, block mass M and stress increase A. Stiffness k_L is related to the spring by which blocks are attached to the upper moving plate, which according to Brown et al. [32] needs to be much more flexible than spring connecting the blocks (whose stiffness is described by k_C), since the distance between the interacting blocks along the fault is much smaller than the dimension of the driving plate. In present analysis if one takes that the value of k_C is around 1, than parameter k_L could take values two order of units smaller, $k_L = 10^{-2}$. This further means that relevant values of parameter c (k_C/k_L) are of 10^2 order of unit. Regarding the block mass, we assume that M takes very small values (order of unit of 10^{-6}), since, in present analysis, we do not analyze the effect of gravity (normal stress), but dynamic instability is assumed to occur due to effect of friction and delayed interaction. Hence, analysis is conducted for almost massless blocks. When all of these assumptions, constraints and previously obtained results are taken into consideration, one arrives at the relevant values of ξ of the order of 10^{-1} (Table 1).

Table 1
Relevant parameter values for the analysis.

Parameter	Relevant value from the previous studies (order of unit)	Reference
Stress increase: A	$10.3 - 19.9 \times 10^{-3}$	[25]
Stress drop: B	$12.1 - 20.3 \times 10^{-3}$	[25]
Spring stiffness between the upper plate and the block: k_L	$k_L << k_C$ (10^{-2})	[26]
Critical slip distance: L	10^{-2}	[27]
Velocity of the driving plate: V_0	1	[16]
	Controlling parameters	
Parameter	Relevant value from the previous studies (order of unit)	Adopted interval for present analysis
$\varepsilon = (B-A) / A$	[−0.17,0.36]	[−1,1]
$\xi = k_L \times M/A$	10^{-1}	[0,1]
$\gamma = (k_L/M)^{1/2} \times (L/V_0)$	1	[0,2]

Relevant values of parameter γ are determined by taking into the consideration the spring stiffness k_L, block mass M, critical slip distance L and velocity of the upper driving plate V_0. According to Scholz [33], critical slip distance L represents a displacement needed to make a transition between the steady-state friction regimes (Fig. 2). Its recommended value is 10^{-2} order of unit. Regarding the velocity of the upper driving plate, V_0, its relevant value is determined by the stationary solution of system (2), which is $(\theta,U,V) = (0,0,1)$ according to Erickson et al. [16]. Hence, we take $V_0 = 1$ as a meaningful value of the upper plate velocity. Concerning these appropriate values of k_L, M, L and V_0, one finds that relevant value of γ is of a single order of unit (Table 1).

One should note that the value of time delay is observed in comparison with the oscillation period relevant from the seismological viewpoint. In present paper, authors consider time delay as relevant for those values which are significantly smaller that the corresponding oscillation period. This is in correspondence with the proposal by Burridge and Knopoff, who took time delay significantly smaller for the part of the fault that exhibits viscous slipping rather that the parts that move by fracture.

4. Results

Regarding the local bifurcation analysis, the considered delay differential equation (DDE) system is treated numerically using DDE BIFTOOL, having the obtained results further corroborated by the Runge-Kutta 4th order numerical method. System (4) has only one stationary solution, namely $(\theta_1,U_1,V_1,\theta_2,U_2,V_2) = (0,0,1,0,0,1)$, which corresponds to steady sliding. We proceed in the standard way to determine and analyze the characteristic equation of (4) around a stationary solution (0,0,1,0,0,1). Details of the analysis are given in Appendix.

Next we shall analyze the effect of stationary time delay coupled with the influence of coupling strength c and the main control parameters of the observed system, namely ε, ξ and γ. All the analyzes were done for the limit cycle as the starting dynamical regime of the initial observed system ($\tau = 0$), which is considered as a co-seismic regime.

Fig. 3 shows the Hopf bifurcation curves in τ-c diagram. For the relevant range of values for coupling strength (10^2 order of unit), observed system exhibit inverse Andronov–Hopf bifurcation, from the initial oscillatory regime, with period T≈12, to equilibrium state (fixed point), for very small value of time delay, $\tau \approx 0.01$. Increase of time delay, e.g. $\tau = 0.3$, for $c = 100$, induces an occurrence of a direct Andronov–Hopf bifurcation, with the appearance of regular periodic oscillations, with period $T = 0.5$. Regarding the oscillation amplitudes, direct Andronov–Hopf bifurcation triggers approximately ten times smaller displacements.

Effect of the interaction of time delay and dimensionless stress ratio ε is given in Fig. 4. As in the previous case, an inverse supercritical Andronov–Hopf bifurcation curve occurs with the increase of τ, introducing the change of dynamical regime from the limit cycle (for the values of $\varepsilon > 0.27$) to equilibrium state, and further again to regular periodic oscillations (for $\tau > 0.3$), with the occurrence of direct bifurcation. Qualitatively similar behavior is observed when τ and nondimensional frequency γ are simultaneously varied (Fig. 5). With the increase of time delay, for constant value of γ, both inverse and direct supercritical Andronov–Hopf bifurcation occurs.

In the case when τ and ξ are varied, while other parameters are held fixed for the equilibrium state of the original system (2),

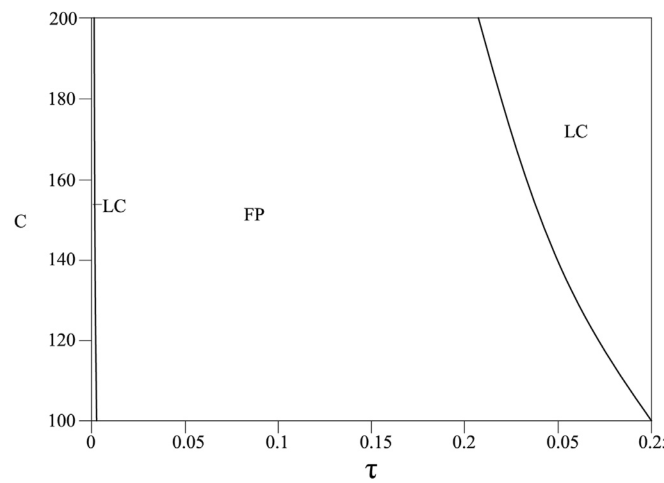

Fig. 3. Diagram $\tau(c)$, for the fixed values of parameters $\varepsilon = 0.4$, $\xi = 0.5$ and $\gamma = 0.8$ (limit cycle of the starting system). Andronov–Hopf bifurcation curves denotes the transition from limit cycle (LC) to equilibrium state (EQ) and again to limit cycle (LC). Qualitatively similar diagrams are obtained for other parameter values for the initial conditions near the equilibrium point.

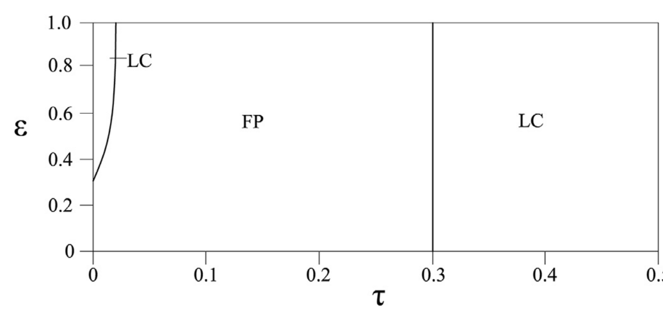

Fig. 4. Diagram $\tau(\varepsilon)$, for the fixed values of parameters $c = 100$, $\xi = 0.5$ and $\gamma = 0.8$ (limit cycle of the starting system). Andronov–Hopf bifurcation curve denotes the transition from the initial limit cycle (LC) across the equilibrium state (EQ) and again to limit cycle (LC). Qualitatively similar diagrams are obtained for other parameter values for the initial conditions near the equilibrium point.

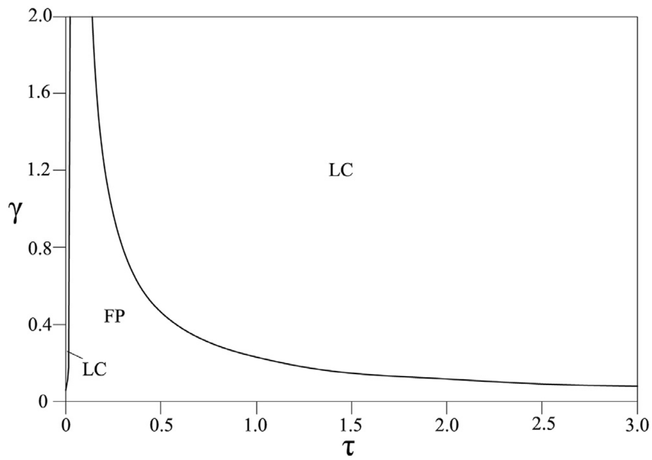

Fig. 5. Diagram $\tau(\gamma)$, for the fixed values of parameters c = 100, $\xi = 0.5$ and $\varepsilon = 0.4$ (limit cycle of the starting system). Andronov–Hopf bifurcation curve denotes the transition from equilibrium state (EQ) to limit cycle (LC). Qualitatively similar diagrams are obtained for other parameter values for the initial conditions near the equilibrium point.

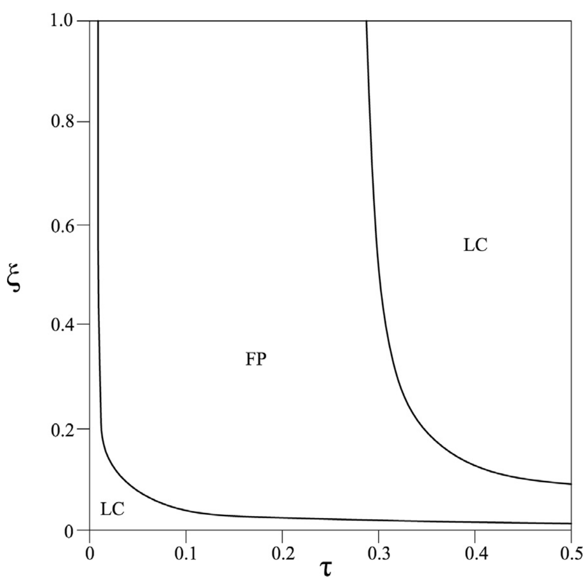

Fig. 6. Diagram $\tau(\xi)$, for the fixed values of parameters c = 100, $\varepsilon = 0.4$ and $\gamma = 0.8$ (limit cycle of the starting system). Andronov–Hopf bifurcation curve denotes the transition from the limit cycle (LC) across the equilibrium state (EQ) to limit cycle (LC). Qualitatively similar diagrams are obtained for other parameter values for the initial conditions near the equilibrium point.

there is an Andronov–Hopf bifurcation curve occurs from the equilibrium state to regular periodic oscillations (Fig. 6).

5. Discussion

Results of the performed analysis are new and meaningful for both the nonlinear dynamics and seismology. From the viewpoint of nonlinear dynamics, present analysis is relevant from the phenomenological aspect. In particular, the obtained results indicate that by assuming the delayed interaction between the blocks, one can observe two phenomena: inverse and direct Andronov–Hopf bifurcation. It should be emphasized that this feature is observed for the values of time delay about 4×10^2 order of unit smaller than the corresponding period of regular oscillations of the starting system (for $\tau \approx 0$).

From the seismological aspect, interpretation could be interesting if one looks in the opposite direction. In particular, if the existence of delayed interaction among different fault segments is justified, considering different viscous properties of fault gouge, than starting dynamical regime should be with introduced positive value of time delay. This means that the starting system is probably in equilibrium state (fixed point), which is proved to occur with the introduction of time delay. However, further increase of time delay induces the transition to regular periodic oscillations, which certainly could not be considered as the onset of co-seismic regime, for two main reasons. Firstly, frequency of displacements is very high, i.e. oscillation period is approximately 0.5, which is near the value of time delay (0.3), where the bifurcation point occurs. Such large value of time delay could hardly be expected in natural conditions. Secondly, displacement amplitude is about ten times smaller than for the starting system, which is also not likely to happen, since the majority of displacement along the fault takes place during the earthquakes, i.e. in the co-seismic regime. Hence, in order to “force” the examined system with the included time delay to enter the co-seismic regime, one needs to analyze the conditions which lead to the reduction of viscosity effect. Certainly, weaker impact of viscosity is expected in high temperature and low pressure conditions, which are the two conditions usually satisfied during the fault movement. In particular, the unconsolidated angular shaped rock material that constitutes the fault gouge exhibits high friction, which further induces the increase in temperature. Also, during the fault movement, fault itself is released of the pressure generated by the strong tectonic forces acting in opposite directions along the fault. In particular, heat generated during frictional sliding is a substantial component of the energy budget of earthquakes [34,35]. When time delay is significantly small ($\tau \ll 0.01$), fault enters the co-seismic dynamical regime, where regular periodic oscillations have low-frequency (i.e. high period, T≈12), and rather large amplitude (around $1.2 - 2.0$ in our numerical simulations). Certainly, case with $\tau = 0$ is out of the question, since main assumption of the analysis is that delayed interaction is inherent property of the compound fault.

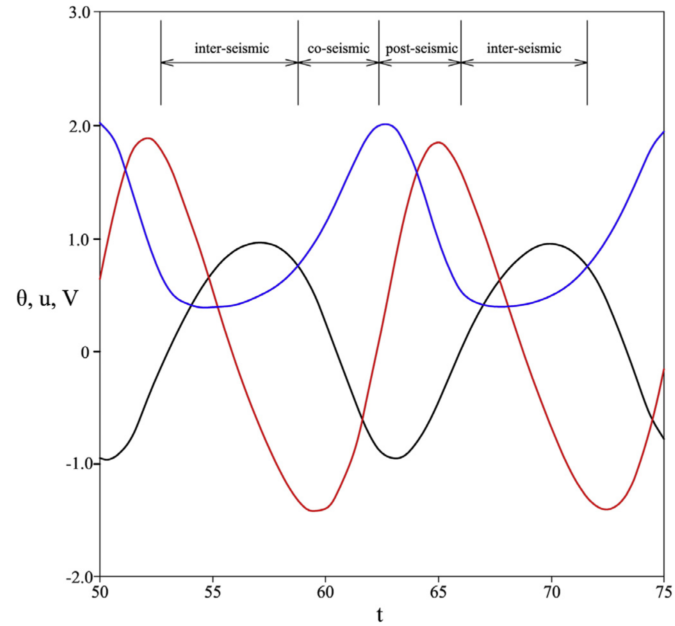

Fig. 7. Transition between seismic cycles in oscillatory regime of spring-slider dynamics. Black line denotes the change of friction (state variable), red line is for displacement, while blue line indicates the change of velocity.

Once the examined model is in oscillatory regime, one could easily recognize the co-seismic, post-seismic and inter-seismic regime, latter of which represent short-term occurrence (Fig. 7).

One should note that such dynamics, relevant from the viewpoint of seismology, is observed for the parameter values adopted using the previous laboratory findings.

6. Conclusion

In present paper, authors examine dynamics of a spring-slider model as a setup of fault movement. Examined model is composed of two blocks with delayed interaction, which mimics delayed interaction among a group of blocks from the original Burridge–Knopoff model. Analysis is conducted for the parameter values relevant from the seismological viewpoint, based on the previous laboratory findings and seismological observations. Main goal of the research was to establish the background dynamics of a seismic cycle, including the transition from steady state or aseismic creep to stick-slip-like seismic regime, with alternation of inter-seismic, co-seismic and post-seismic cycles.

Results of the performed analysis indicate the following. Introduction of small time delay, significantly smaller when compared to the period of oscillatory regime, leads to transition from fixed point (equilibrium state) to periodic oscillations (limit cycle). From the viewpoint of seismology, these findings indicate a key role of the interaction among different parts of a compound fault in generation of seismogenic motion. More closely, effect of viscosity of a fault zone plays a crucial role in transmission of a movement along the fault. From the standpoint of earthquake phenomenology, one could consider regular periodic oscillations as an example of stick-slip like regime, with the successive shifts between the co-seismic regime (increasing velocity branch and decreasing friction), post-seismic regime (decreasing velocity branch and increasing friction) and inter-seismic regime (quasi-stationary velocity branch). On the other hand, some authors could consider the whole oscillatory regime as a representative of a co-seismic fault movement [36].

Another interesting outcome of the present research lies in the specific effect of the main controlling parameters, which were previously indicated as the most relevant for the modeled fault dynamics [16]. Apparently, ratio of stress drop to stress increase (parameter ε), for the range of other parameters' values relevant from the seismological viewpoint and for the assumed delayed interaction as inherent property of fault dynamics, induces the transition from equilibrium state to periodic oscillations. Regarding the effect of other two parameters, γ and ξ, related to the stiffness of the spring connecting the blocks and the upper driving plate, results obtained imply that a change from steady state or aseismic creep to seismic fault motion occurs with the increase of γ and ξ. However, these parameters are considered as constants for the observed system, so it is highly unlikely to expect their significant changes during the fault motion. The expected changes of these parameters are either small or these changes are slow from the viewpoint relevant for the duration of seismogenic fault motion.

As for the effect of coupling strength c, increase of c for the relevant range of parameter values ($>10^2$) leads to the change of dynamical regime only for rather high values of time delay, which is certainly not expected in the real conditions along the fault zone in the Earth's crust. Hence, in this case, time delay plays again the significant role, in a way that the reduction of time delay could lead to the onset of co-seismic regime.

Concerning the predominant effect of delayed coupling on dynamics of fault motion, further research could include the analysis of time varying delay on fault motion. Such an assumption is justified from the seismological viewpoint, since one could expect changes of friction properties along the fault zone in a reasonable period of time. From the standpoint of nonlinear dynamics, introduction of coupling with variable delay would certainly induce more complex behavior and, maybe, indicate some new dynamical mechanisms in the background of earthquake nucleation.

Acknowledgments

This research was partly supported by the Ministry of Education, Science and Technological Development of the Republic of Serbia (Contract Nos. 176016 and 171017).

Appendix

Linearization of the system (4) and substitution $\theta_1 = A_1 e^{\lambda t}$, $U_1 = B_1 e^{\lambda t}$, $V_1 = C_1 e^{\lambda t}$, $\theta_2 = A_2 e^{\lambda t}$, $U_2 = B_2 e^{\lambda t}$, $V_2 = C_2 e^{\lambda t}$ and with $U_1(t\text{-}\tau) = B_1 e^{\lambda(t\text{-}\tau)}$ and $U_2(t\text{-}\tau) = B_2 e^{\lambda(t\text{-}\tau)}$ results in a system of algebraic equations for the constants A_1, B_1, C_1, A_2, B_2 and C_2. This system has a nontrivial solution if the following is satisfied:

$$\begin{aligned} &-(\lambda+1)\left[\lambda\left(\lambda+\gamma_1^2\left(\frac{1}{\xi_1}\right)\right)\cdot D\right. \\ &\left.+\gamma_1^2(1+c_1)\cdot D+\gamma_1^2 c_1 e^{-\lambda\tau}(\lambda+1)\gamma_2^2 c_2 e^{-\lambda\tau}\right] \\ &+\lambda(1+\varepsilon_1)\gamma_1^2\left(\frac{1}{\xi_1}\right)\cdot D=0 \end{aligned} \tag{1A}$$

where:

$$D=\begin{vmatrix} -(\lambda+1) & 0 & -(1+\varepsilon_2) \\ 0 & -\lambda & 1 \\ -\gamma_2^2\left(\frac{1}{\xi_2}\right) & -\gamma_2^2(1+c_2) & -\left(\lambda+\gamma_2^2\left(\frac{1}{\xi_2}\right)\right) \end{vmatrix}$$

The Eq. (1A) is the characteristic equation of the system (4) and can be written in the following form:

$$\begin{aligned} &\left\{-(\lambda+1)\left[\lambda\left(\lambda+\gamma_1^2\left(\frac{1}{\xi_1}\right)\right)+\gamma_1^2(1+c_1)\right]+\lambda(1+\varepsilon_1)\gamma_1^2\left(\frac{1}{\xi_1}\right)\right\}\cdot \\ &D=(\lambda+1)^2\gamma_1^2\gamma_2^2 c_1 c_2 e^{-2\lambda\tau} \end{aligned} \tag{2A}$$

in which we substitute $\lambda = i\omega$ to obtain:

$$\begin{aligned} &\frac{\left\{\left[\omega^2\gamma_1^2\left(\frac{1}{\xi_1}\right)+\omega^2-\gamma_1^2(1+c_1)\right]+i\omega\left[\omega^2-\gamma_1^2(1+c_1)-\gamma_1^2\left(\frac{1}{\xi_1}\right)+(1+\varepsilon_1)\gamma_1^2\left(\frac{1}{\xi_1}\right)\right]\right\}D}{\gamma_1^2\gamma_2^2 c_1 c_2\left[-\omega^2+1+i2\omega\right]}= \\ &=\cos(2\omega\tau)-i\sin(2\omega\tau) \end{aligned} \tag{3A}$$

The resulting two equations for the real and imaginary part of (3A) after squaring and adding give an equation for each of the parameters, c_1, c_2, ε_1 and ε_2 in terms of the other parameters, ω, μ, γ_1 and γ_2, and after division, an equation for τ in terms of the parameters ω, μ, γ_1, γ_2, ε_1, ε_2, ξ_1 and ξ_2. In this way, one obtains parametric representations of the relations between τ and the parameters, which correspond to the bifurcation values $\lambda = i\omega$. The general form of such relations is illustrated by the following formula for ε_1 as a function of ω:

$$(1+\varepsilon_1)_{1/2} = -\frac{F \pm \sqrt{F^2 - G^2}}{H} \tag{4A}$$

where F, G and H are abbreviations for the following terms:

$$\begin{aligned} F=&\left(\omega\left[\left(\omega^2-\gamma_1^2(1+c_1)-\gamma_1^2\left(\frac{1}{\xi_1}\right)\right)B+AD\right]\left(-\omega^2+1\right)\right. \\ &\left.-2\left[AB-\omega^2\left(\omega^2-\gamma_1^2(1+c_1)-\gamma_1^2\left(\frac{1}{\xi_1}\right)\right)D\right]\right)\cdot \\ &\omega\gamma_1^2\left(\frac{1}{\xi_1}\right)\left\{B\left(-\omega^2+1\right)+2\omega^2 D\right\} \\ &+\left(\left(AB-\omega^2\left(\omega^2-\gamma_1^2(1+c_1)-D\gamma_1^2\left(\frac{1}{\xi_1}\right)\right)\right)\left(-\omega^2+1\right)\right. \\ &\left.+B\omega^2\left(2\left(\omega^2-\gamma_1^2(1+c_1)-\gamma_1^2\left(\frac{1}{\xi_1}\right)\right)+AD\right)\right) \end{aligned}$$

$$G = \left[\left(\omega \gamma_1^2 \left(\frac{1}{\xi_1} \right) \left\{ B\left(-\omega^2+1\right) + 2\omega^2 D \right\} \right)^2 + \left(\omega^2 \gamma_1^2 \left(\frac{1}{\xi_1} \right) \left\{ B\left(1+\frac{1}{\mu}\right) - D\left(-\omega^2+1\right) \right\} \right)^2 \right] \cdot$$
$$\left[\left(\left(\omega \left[\left(\omega^2 - \gamma_1^2(1+c_1) - B\gamma_1^2\left(\frac{1}{\xi_1}\right)\right) + AD \right] \left(-\omega^2+1\right) - 2\left[AB - D\omega^2 \left(\omega^2 - \gamma_1^2(1+c_1) - \gamma_1^2\left(\frac{1}{\xi_1}\right)\right)\right]\right)\right)^2 + \right.$$
$$+ \left(\left(AB - \omega^2 \left(\omega^2 - \gamma_1^2(1+c_1) - D\gamma_1^2\left(\frac{1}{\xi_1}\right)\right)\right)\left(-\omega^2+1\right) + \omega^2 \left(2\left(\omega^2 - \gamma_1^2(1+c_1) - B\gamma_1^2\left(\frac{1}{\xi_1}\right)\right) + AD \right)\right)^2 -$$
$$\left. - \left(\left(\left(-\omega^2+1\right)^2 + 2\omega^2 \right) \left(\gamma_1^2 \gamma_2^2 c_1 c_2 \right) \right)^2 \right]$$

$$H = \left(\gamma_1^2 \left(\frac{1}{\xi_1} \right) \omega \left\{ B\left(-\omega^2+1\right) + 2\omega^2 D \right\} \right)^2 + \left(\omega^2 \gamma_1^2 \left(\frac{1}{\xi_1} \right) \left\{ 2B - D\left(-\omega^2+1\right) \right\} \right)^2 \quad (5A)$$

and A, B and D are:

$$A = \omega^2 \gamma_1^2 \left(\frac{1}{\xi_1} \right) + \omega^2 - \gamma_1^2 (1+c_1)$$
$$B = \omega^2 \cdot \left(\gamma_2^2 \left(\frac{1}{\xi_2} \right) + 1 \right) - \gamma_2^2 (1+c_2) \quad (6A)$$
$$D = \omega^2 - \gamma_2^2 (1+c_2) - \gamma_2^2 \left(\frac{1}{\xi_2} \right) + \gamma_2^2 (1+\varepsilon_2) \left(\frac{1}{\xi_2} \right)$$

On the other hand, for c_1 as a function of ω:

$$(c_1)_{1/2} = \frac{-F \pm \sqrt{F^2 - GH}}{H} \quad (7A)$$

where F,G and H are the same as in (7).

For τ as a function of ω:

$$\tau = \frac{1}{2\omega} \left\{ \arctan\left(-\frac{J}{K} \right) + k\pi \right\} \quad (8A)$$

where k is any nonnegative integer such that $\tau_k \geq 0$, and J and K are the abbreviations for the following terms:

$$J = \frac{\omega}{\left(-\omega^2+1\right)^2 + 4\omega^2} \left\{ [CB+AD]\left(-\omega^2+1\right) - \left[2AB - \omega^2 CD\right] \right\}$$
$$K = \frac{1}{\left(-\omega^2+1\right)^2 + 4\omega^2} \left\{ \left[AB - \omega^2 CD\right]\left(-\omega^2+1\right) + 2\omega^2 [CB+AD] \right\} \quad (9A)$$

where A, B and D are the same as in (8), and C stands for the following term:

$$C = \omega^2 - \gamma_1^2 (1+c_1) - \gamma_1^2 \left(\frac{1}{\xi_1} \right) + (1+\varepsilon_1) \gamma_1^2 \left(\frac{1}{\xi_1} \right). \quad (10A)$$

References

[1] Ayyub BM, McCuen RH. Probability, statistics and reliability for engineers and scientists. Boca Raton, Florida, USA: CRC Press; 2000. p. 628.
[2] Ito T, Hashimoto M. Spatiotemporal distribution of interplate coupling in southwest Japan from inversion of geodetic data. J Geophys Res 2004:109.
[3] Thatcher W. The earthquake deformation cycle at the Nankai trough, southwest Japan. J Geophys Res 1984;89:3087–101.
[4] Jonsson S, Segall P, Pedersen R, Bjornsson G. Post-earthquake ground movements correlated to pore-pressure transients. Nature 2003;424:179–83.
[5] Scholz CH. Earthquakes and friction laws. Nature 1998;391:37–42.
[6] Hetland EA, Hager BH. Postseismic relaxation across the central Nevada seismic belt. J Geophys Res 2003;108. doi:10.1029/2002JB002257.
[7] Brace WF, Byerlee JD. Stick-slip as a mechanism for earthquakes. Science 1966;153(3739):990–2.
[8] Byerlee JD. The mechanics of stick-slip. Tectonophys 1970;9(5):475–86.
[9] Gobel THW. Microseismicity, fault structure, & the seismic cycle. University of Southern California; 2013. p. 172.
[10] Burridge R, Knopoff L. Model and theoretical seismicity. Bull Seismol Soc Am 1967;57(3):341–71.
[11] Winter ME. The plausibility of long-wavelength stress correlation or stress magnitude as a mechanism for precursory seismicity: results from two simple elastic models. Pure Appl Geophys 2000;157(11-12):2227–48.
[12] Mori T, Kawamura H. Spatiotemporal correlations of earthquakes in the continuum limit of the one-dimensional Burridge–Knopoff model. J Geophys Res 2008;113(11):B11305.
[13] Amundsen DS, Scheibert J, Thøgersen K, Trømborg J, Malthe-Sørenssen A. 1D model of precursors to frictional stick-slip motion allowing for robust comparison with experiments. Tribol Lett 2012;45(2):357–69.
[14] Ichinose S. Non-equilibrium statistical approach to friction models. Tribol Int 2016;93:446–50.
[15] Ueda Y, Morimoto S, Kakui S, Yamamoto T, Kawamura H. Dynamics of earthquake nucleation process represented by the Burridge–Knopoff model. Eur Phys J B 2015;88(9):235.
[16] Erickson B, Birnir B, Lavallee D. A model for aperiodicity in earthquakes. Nonlinear Process Geophys 2008;15:1–12.
[17] Caldeira B, Silva HG, Borges JF, Tlemçani M, Bezzeghoud M. Chaotic behavior of seismic mechanisms: experiment and observation. Ann Geophys 2012;55(1):57–62.
[18] Kostić S, Franović I, Perc M, Vasović N, Todorović K. Triggered dynamics in a model of different creep regimes, 4. Scientific Reports: Nature Publishing Group; 2014. p. 5401.
[19] Valipour M, Asghar Montazar A. An evaluation of SWDC and WinSRFR models to optimize of infiltration parameters in furrow irrigation. American J Sci Res 2012;69:128–42.
[20] Valipour M. Increasing irrigation efficiency by management strategies: cutback and surge irrigation. ARPN J Agri Biol Sci 2013;8:35–43.
[21] Valipour M. Application of new mass transfer formulae for computation of evapotranspiration. J Appl Water Eng Res 2014;2:33–46.
[22] Valipour M. Use of surface water supply index to assessing of water resources management in Colorado and Oregon, US. Adv Agri Sci Engineering Res 2013;3:631–40.
[23] Valipour M, Ali Gholami Defidkouhi M, Raeini Sarjaz M. Selecting the best model to estimate potential evapotranspiration with respect to climate change and magnitudes of extreme events. Agri Water Manage 2017;180:50–60.
[24] Valipour M. Number of required observation data for rainfall forecasting according to the climate conditions. Am J Sci Res 2012;74:79–86.
[25] Kostić S, Franović I, Todorović K, Vasović N. Friction memory effect in complex dynamics of earthquake model. Nonlinear Dyn 2013;73(3):1933–43.
[26] Kostić S, Vasović N, Franović I, Todorović K. Dynamics of simple earthquake model with time delay and variation of friction strength. Nonlinear Process Geophys 2013;20:857–65.
[27] Vasović N, Kostić S, Franović I, Todorović K. Earthquake nucleation in a stochastic fault model of globally coupled units with interaction delays. Commun Nonlinear Sci Numer Simul 2016;38:117–29.
[28] Scholz CH. The mechanics of earthquake and faulting. Cambridge: Cambridge University Press; 2002. p. 504.
[29] Dieterich JH, Kilgore BD. Direct observation of frictional contacts: new insights for state dependent properties. Pure Appl Geophys 1994;143:283–302.
[30] Clancy I, Corcoran D. State-variable friction for the Burridge–Knopoff model. Phys Rev E Stat Nonlin Soft Matter Phys 2009;80:016113.
[31] Kilgore BD, Blanpied ML, Dieterich JH. Velocity dependent friction of granite over a wide range of conditions. Geophys Res Lett 1993;20:903–6.
[32] Brown SR, Scholz CH, Rundle JB. A simplified spring-block model of earthquakes. Geophys Res Lett 1991;18:215–18.
[33] Scholz CH. The critical slip distance for seismic faulting. Nature 1988;336:761–3.
[34] McGarr A, Fletcher JB, Beeler NM. Attempting to bridge the gap between laboratory and seismic estimates of fracture energy. Geophys Res Lett 2004;31:L14606. doi:10.1029/2004GL020091.
[35] Venkataraman A, Kanamori H. Observational constraints on the fracture energy of subduction zone earthquakes. J Geophys Res 2004;109:B05302. doi:10/1019/2003JB002549.
[36] Vasudevan K, Cavers M, Ware A. Earthquake sequencing: chimera states with Kuramoto model dynamics on directed graphs. Nonlinear Process Geophys 2015;22:499–512.